Plasmonic quantum dot solar cells for enhanced infrared response

Hao Feng Lu, Sudha Mokkapati, Lan Fu, Greg Jolley, Hark Hoe Tan et al.

Citation: Appl. Phys. Lett. **100**, 103505 (2012); doi: 10.1063/1.3691917
View online: http://dx.doi.org/10.1063/1.3691917
View Table of Contents: http://apl.aip.org/resource/1/APPLAB/v100/i10
Published by the American Institute of Physics.

Plasmonic quantum dot solar cells for enhanced infrared response

Hao Feng Lu,[a] Sudha Mokkapati, Lan Fu, Greg Jolley, Hark Hoe Tan, and Chennupati Jagadish
Department of Electronic Materials Engineering, Research School of Physics and Engineering, The Australian National University, Canberra ACT 0200, Australia

(Received 25 November 2011; accepted 11 February 2012; published online 7 March 2012)

Enhanced near infrared photoresponse in plasmonic InGaAs/GaAs quantum dot solar cells (QDSC) is demonstrated. Long wavelength light absorption in the wetting-layer and quantum-dot region of the quantum dot solar cell is enhanced through scattering of light by silver nanoparticles deposited on the solar cell surface. Plasmonic light trapping results in simultaneous increase in short-circuit current density by 5.3% and open circuit voltage by 0.9% in the QDSC, leading to an overall efficiency enhancement of 7.6%. © *2012 American Institute of Physics*. [http://dx.doi.org/10.1063/1.3691917]

Bringing down the cost of electricity generated from solar radiation using photovoltaics (PV) has been the focus of intense investigations in recent years. Along with the ongoing research and industry development to reduce the cost of conventional PV devices such as Si-based solar cells, significant research efforts have been focused on exploring new concepts and approaches for high efficiency solar cells, especially through the fast emerging nanotechnology to exploit the unique properties of nanostructures[1] such as self-assembled quantum dots (QDs). By incorporating self-assembled QDs into the intrinsic region of a standard p-i-n solar cell structure during the epitaxial growth, photons in the solar spectrum with energy lower than the energy gap of the bulk host material can be absorbed by the QD layers, leading to an extended photoresponse into longer wavelengths and hence larger photocurrent. Different QD systems based on GaAs p-i-n structures have been investigated,[2–5] with the demonstration of improved short circuit current density (J_{sc}) (compared with the GaAs reference cell). Quantum dot solar cells (QDSCs) have also shown promise in further improving the performance of the most efficient multi-junction solar cell devices due to the flexibility in bandgap engineering. For example, InAs QDs have been incorporated into the middle InGaAs sub-cell of an AlGaInP/InGaAs/Ge multi-junction solar cell. The QD layers increase the absorption of the middle sub-cell, shifting carrier generation from the current over-producing bottom sub-cell to the current under-producing middle sub-cell. This provides better current-matching and hence the improved output current of the entire device, leading to efficiencies >40% under solar concentration using flash simulators.[6]

Even though QDs extend the photoresponse of solar cells into the long wavelength region,[7] their contribution to J_{sc} is still very small due to very small QD absorption cross section. While an increase in J_{sc} has been demonstrated in various studies via QD/barrier doping[8,9] or by incorporating a large number of QD layers,[10,11] maintaining similar values of open circuit voltage (V_{oc}) in QDSC (to that of reference GaAs solar cell) seems to be a challenge even for the best reported QDSCs.[4,8,12] The former approach requires careful and extensive optimization of epitaxial growth conditions, and increasing the number of QD layers tends to result in strain accumulation and increased defects within the QDs and thus poorer over-all device performance. Hence, enhancing the QD absorption to increase J_{sc} without reduction of V_{oc} becomes critical for achieving QDSC with high efficiency.

In this work, we propose to enhance the long wavelength photon absorption of the QDSCs by employing light trapping. Light trapping refers to the phenomenon of increasing the path length of light and hence total absorption inside a thin absorber layer. Light trapping can be achieved by depositing metal nanoparticles on the solar cell surface. The light incident on the nanoparticles is scattered strongly due to excitation of localized surface plasmons. A fraction of scattered light is coupled into the solar cell. The nanoparticles scatter light at random angles and the light coupled into the cell at angles greater than the critical angle for total internal reflection at the cell/air interface is trapped inside the cell, and results in enhanced absorption in the cell (in the far-field of the nanoparticles). Plasmonic light trapping can be incorporated into the solar cells after the general device fabrication sequence and does not alter the basic device structure/processing steps. Enhancement of absorption in a thin absorber using plasmonics was demonstrated by Stuart and Hall[13] and has been extensively studied since then.[14–16] Due to direct bandgap of GaAs, light trapping is not necessary for bulk GaAs solar cells. However, it becomes critical for III-V based thin film or quantum well solar cells or QDSCs due to the very thin (thinner than the absorption length) absorber layers. Enhanced performance of GaAs thin film solar cells due to plasmonic light trapping and InP/InGaAsP quantum-well solar cells due to nanoparticle light scattering have been demonstrated.[17,18] Investigating plasmonic light trapping for high efficiency QDSCs is the subject of this study.

Light trapping can be achieved by depositing metal nanoparticles either on the front or on the rear of the solar cell. Below the particle plasmon resonance frequency, light scattered by the nanoparticles is in phase with respect to the incident light, whereas for higher frequencies (shorter wavelengths), the light scattered by the nanoparticles is out of phase with respect to the incident light.[16,19] When nanoparticles are deposited on the illuminated (front) surface of the solar cell, due to the phase difference, interference between

[a]Electronic mail: hfl109@physics.anu.edu.au.

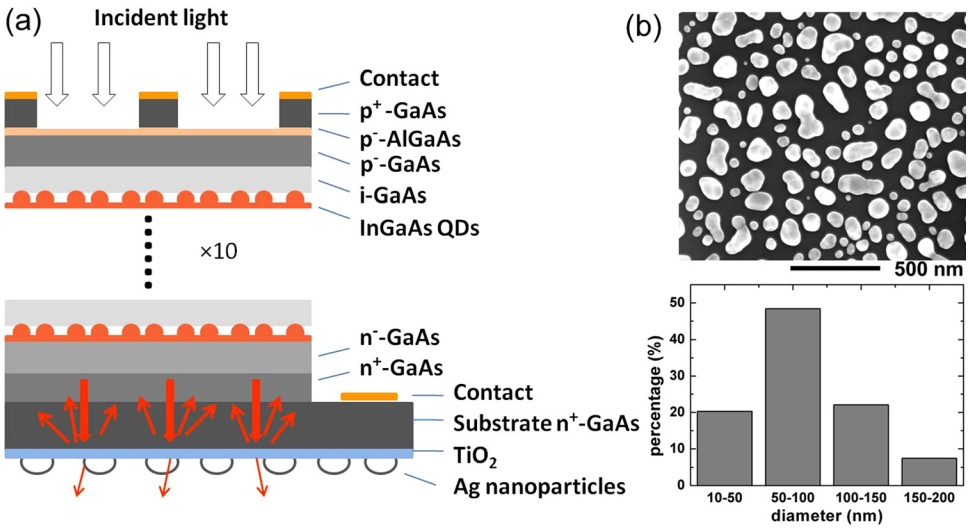

FIG. 1. (Color online) (a) Schematic of the InGaAs/GaAs QD solar cell structure used in this study. (b) SEM image of the nanoparticles formed on the rear of the solar cells and their size distribution.

light directly transmitted into the solar cell (without interaction with the nanoparticles) and light scattered into the solar cell by the nanoparticles leads to lower net intensity inside the solar cell for frequencies higher than the particle plasmon resonance frequency.[19] Lower net intensity of short wavelength light inside the solar cell degrades the photoresponse of the cell in the short wavelength region, resulting in reduced J_{sc}. However, if the nanoparticles are deposited on the rear of the solar cell,[20] the short wavelength light is absorbed in the bulk GaAs layers in a single pass before it reaches the rear surface and interacts with the nanoparticles. Only the long wavelength light (with energy lower than the bandgap of GaAs) that is not completely absorbed in the solar cell in the first pass interacts with the nanoparticles and is scattered back into the solar cell leading to enhanced path length. Enhanced path length for the long wavelength light increases the absorption in the QD layer. For this reason, we study nanoparticle arrays on the rear of the solar cell.

Figure 1(a) shows a schematic of the p-i-n QDSC structure used for this study. The structure was grown on n^+-GaAs (001) substrate using metal-organic chemical vapor deposition (MOCVD). The intrinsic layer of the devices consisted of ten layers of 5 monolayer thick $In_{0.5}Ga_{0.5}As$ QDs with 50-nm-thick GaAs barrier layers. The QD density for each layer was $\sim 4.5 \times 10^{10}\,cm^{-2}$. Si and Zn were used as n- and p-type dopants for the contact layers. 850 μm diameter circular devices were fabricated by depositing both n- and p-type contacts on the top side of the wafer. After metallization of contacts, 100 nm of heavily p-doped GaAs layer on the illuminated surface of the solar cell was etched away to reduce absorption and recombination.

The localized surface plasmon resonance of the nanoparticle can be tuned to the bandgap of QDs by depositing them directly on GaAs substrates. However, deposition directly on GaAs resulted in very large and highly non-uniform particle arrays. Following device fabrication, the rear of the wafers were mechanically polished and coated with 5, 10, or 20 nm thick TiO_2 layer using atomic layer deposition (ALD). TiO_2 was chosen as the spacer layer material because of its higher refractive index, necessary for tuning the particle plasmon resonance closer to the band edge of QDs, without increasing the nanoparticle size. 18 nm thick Ag film was evaporated on the TiO_2 layer and the samples were annealed in N_2 at 200 °C for 50 min. As a result the Ag film formed into nanoparticles with some degree of size dispersion, as shown in Fig. 1(b). The nanoparticles have an average diameter of 120 nm. After deposition of the nanoparticles, the QDSCs were characterized by spectral response and I-V measurements.

The spectral response of a reference QDSC and the plasmonic QDSC are shown in Fig. 2. The response of the cells is normalized to the peak response at ~850 nm. The photocurrent up to ~870 nm is due to absorption in the bulk GaAs. Due to strong absorption in bulk GaAs, light with energy greater than the bandgap of GaAs is absorbed completely in a single pass through the cell and does not interact with the nanoparticles on the rear of the cell. All the solar cell structures investigated here have shown similar GaAs photoresponse signal, and normalizing the photocurrent response of different cells to GaAs photoresponse allows us to compare the QD response from different plasmonic structures. The photocurrent response from the wetting layer (WL) and the QD layer is enhanced in cells with plasmonic structures.

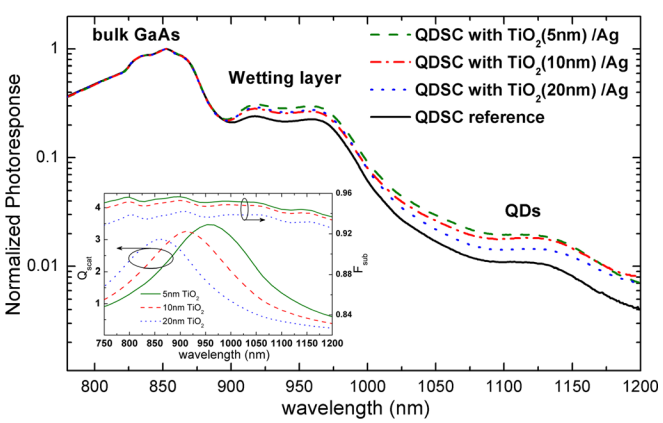

FIG. 2. (Color online) Normalized photocurrent spectral response of the reference QDSC and QDSCs with Ag nanoparticles. The TiO_2 spacer layer thickness is 5, 10, or 20 nm. The photoresponse of the cells is normalized. Inset shows the scattering cross-section, normalized to the cross-sectional area (Q_{scat}), and fraction of scattered light coupled into the substrate (F_{sub}) for a 120 nm diameter Ag hemisphere on GaAs substrate with varying thickness of TiO_2 layer.

TABLE I. Device performance parameters for the QD solar cells with different spacer (TiO_2) thickness, before (underlined numbers in italics) and after deposition of the plasmonic nanoparticles.

	J_{sc} (mA/cm^2)	J_{sc} enhancement (%)	V_{oc} (V)	V_{oc} enhancement (%)	η enhancement (%)
5 nm spacer	***17.76*** 18.70	5.3	***0.769*** 0.776	0.9	7.6
10 nm spacer	***17.83*** 18.65	4.6	***0.756*** 0.762	0.8	5.9
20 nm spacer	***17.52*** 18.15	3.6	***0.772*** 0.780	1.0	4.1

Inset of Fig. 2 shows the calculated normalized (to the particle cross-sectional area) scattering cross-sections (Q_{scat}) and the fraction of scattered light coupled into the substrate (F_{sub}) for 120 nm diameter hemispherical Ag nanoparticles on GaAs substrate for different spacer layer thickness. The data was obtained by simulating a single nanoparticle using commercially available software (Lumerical). The simulations do not account for randomness in the array but do give a qualitative insight into the effect of variations in the spacer layer on the light trapping behavior of the array.[20] Fraction of scattered light coupled into the substrate is determined by calculating the ratio of power scattered into the substrate to the total power scattered (into air and into the substrate) by the particle. The scattering cross section of the nanoparticles increases in magnitude and redshifts to longer wavelengths with decreasing the spacer layer thickness. The fraction of scattered power coupled into the substrate is highest at all wavelengths, as shown in the inset for the 5 nm spacer layer. The proximity of a high refractive index substrate affects the peak position of the particle scattering cross section by modifying the polarizability of the particles due to dynamic depolarization effects.[21] The effect of high index substrates on the scattering cross section of nanoparticles has been widely reported.[20,22] Thinner spacer layer ensures high overlap between the nanoparticle near field and the substrate. High near field overlap increases the field that drives the dipole oscillations in the nanoparticles, leading to an increase in the magnitude of scattering intensity from the nanoparticles,[23] and it also results in better coupling of scattered light into the substrate.[24] For optimal device performance, the nanoparticle scattering cross section and fraction of scattered light coupled into the substrate should be the highest around the QD absorption energy to ensure that most of the light incident on the nanoparticles at these wavelengths is efficiently scattered and coupled into the solar cell. Consistent with the simulation results in the inset of Fig. 2 that show increased scattering cross-section (closer to the bandgap of WL and QDs) and better coupling of scattered light into the substrate for the 5 nm TiO_2 spacer layer, highest enhancement of QDSC spectral response by 35.7% in the 900–1200 nm range is observed experimentally.

Table I shows the J_{sc} and V_{oc} for the QDSCs before and after deposition of the plasmonic nanoparticles determined by measuring the I-V characteristics under standard AM 1.5 G solar irradiation. Measurements on the same cell were conducted just prior to deposition of the nanoparticles to ensure that the variation in J_{sc} and V_{oc} is entirely due to the nanoparticles and not due to variation in device performance across the wafer. The plasmonic solar cell with 5 nm TiO_2 spacer layer results in 5.3% enhancement in J_{sc} and 0.9% enhancement in V_{oc} with respect to the reference solar cell, leading to a corresponding efficiency (η) enhancement of 7.6%. J_{sc} enhancement in the plasmonic solar cells is due to enhanced absorption (and hence photoresponse, as shown in Fig. 2) in the WL and QD regions. Alternative approaches to increasing the absorption of long wavelength light, like increasing the number of QD layers[10,11] or QD/barrier doping,[8,9] have led to inconsistent influence on V_{oc} which does not follow the diode equation. This effect is possibly due to the variation in dot properties in different QDSC structures. Contrary to this, our plasmonic solar cells exhibit increase in V_{oc} which is consistent with the enhancement predicted using the measured J_{sc} enhancement and the diode equation. The simultaneous enhancement in both J_{sc} and V_{oc} observed here is significant for QDSC improvement exploration, which is essential for high efficiency QDSCs.

The path length enhancement of long wavelength light due to scattering by the plasmonic structures is estimated from the photocurrent enhancement. At 1000 nm, the path length enhancement is ~2.1 for the best plasmonic solar cell studied here. The estimated path length enhancement is much lower than the ideal enhancement of $4n^2$ (n being the refractive index of absorbing layer) expected by using perfectly randomizing surfaces.[25] Theoretically, a path length enhancement of 2 is expected by using a reflector behind the solar cell. To evaluate the quality of plasmonic light trapping in our solar cells, we measured the photoresponse from a reference solar cell with a back reflector (Fig. 3(a)). The plasmonic structure does result in much higher absorption in the WL/QD region than is obtained by using a back reflector.

In order to further investigate lower than expected path length enhancement using a back reflector or plasmonic structure, we investigated the photoresponse of the reference solar cell for front and rear illumination configuration. Figure 3(b) shows the schematic of the experimental set-up (in the inset) and the photoresponse of the solar cell. The difference in the photoresponse from the WL/QD region for the front and rear illumination configurations represents the free-carrier absorption in the n^+ doped substrate. For the front illumination configuration, light is incident on the WL/QD region first before passing through the substrate. For the rear illumination configuration, light is attenuated by free-carrier absorption in the substrate before it reaches the WL/QD region. Reduction in the WL/QD photoresponse for the rear illumination configuration indicates significant free carrier absorption in the n^+ substrate of our device structures. Previous studies[26] have also reported significant free carrier absorption in GaAs at ~1000 nm when dopant density is above 1×10^{18} cm^{-3}. It is clear that free carrier absorption is responsible for lower than theoretically expected path length enhancements observed in our devices (QDSC cells with a rear reflector or the plasmonic structures). It has been shown

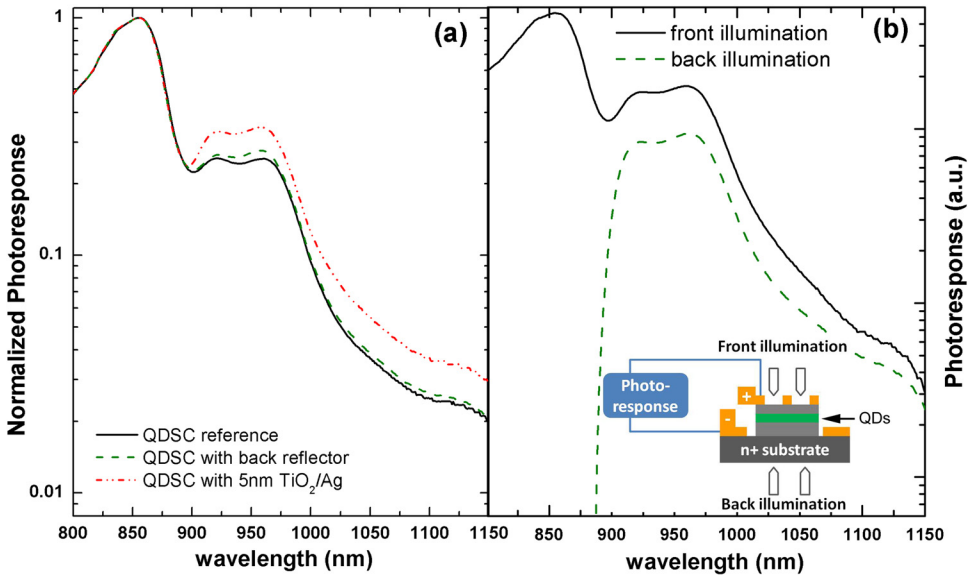

FIG. 3. (Color online) (a) Normalized photoresponse of reference solar cell, reference solar cell with a back reflector and a plasmonic solar cell with 5 nm TiO_2 spacer layer. (b) Photoresponse of the reference QD solar cell under front and rear illumination. Inset shows the illumination configuration.

in Ref. 26 that the absorption coefficient of the semi-insulating GaAs is about 2 orders of magnitude lower than that of n^+ substrate. Hence, it is expected that growing device structures on semi-insulating substrates will significantly reduce the effect of free carrier absorption and will be investigated in future studies.

In summary, we have demonstrated increased IR photoresponse of QD solar cells by incorporating plasmonic nanoparticles on the rear of the solar cell for trapping long wavelength light in the absorbing layer. Contrary to alternative approaches for enhancing QD absorption, our approach does not reduce V_{oc} of the solar cell compared to the reference structure. We demonstrate simultaneous increase in J_{sc} and V_{oc} of up to 5.3% and 0.9%, respectively, with respect to the reference structure. The corresponding efficiency enhancement is 7.6%. The path length enhancement measured in this study is limited by free carrier absorption in the n^+ substrate. Further increase in efficiency enhancement is expected by incorporating the quantum dot structures into device structures grown on semi-insulating substrates.

This work was supported by the Australian Research Council (Grant No. DP1096361). Facilities used in this work are supported by the Australian National Fabrication Facility (ACT node).

[1]T. K. Manna and S. M. Mahajan, in International Conference on Clean Electrical Power, Capri, May 21-23, 2007, p. 379.
[2]R. B. Laghumavarapu, A. Moscho, A. Khoshakhlagh, M. El-Emawy, L. F. Lester, and D. L. Huffaker, Appl. Phys. Lett. **90**, 173125 (2007).
[3]Y. Okada, R. Oshima, and A. Takata, J. Appl. Phys. **106**, 024306 (2009).
[4]D. Guimard, R. Morihara, D. Bordel, K. Tanabe, Y. Wakayama, M. Nishioka, and Y. Arakawa, Appl. Phys. Lett. **96**, 203507 (2010).
[5]H. F. Lu, L. Fu, G. Jolley, H. H. Tan, S. R. Tatavarti, and C. Jagadish, Appl. Phys. Lett. **98**, 183509 (2011).
[6]C. E. Valdivia, S. Chow, S. Fafard, O. Theriault, M. Yandt, J. F. Wheeldon, A. J. SpringThorpe, B. Rioux, D. McMeekin, D. Masson, B. Riel, V. Aimez, R. Ares, J. Cook, T. J. Hall, F. Shepherd, and K. Hinzer, in Conference Record of the 35th IEEE Photovoltaic Specialists Conference, New York, June 20-25, 2010, p. 1253.
[7]G. Jolley, H. F. Lu, L. Fu, H. H. Tan, and C. Jagadish, Appl. Phys. Lett. **97**, 123505 (2010).
[8]K. A. Sablon, J. W. Little, V. Mitin, A. Sergeev, N. Vagidov, and K. Reinhardt, Nano Lett. **11**, 2311 (2011).
[9]T. Morioka, R. Oshima, A. Takata, Y. Shoji, T. Inoue, T. Kita, and Y. Okada, in Conference Record of the 35th IEEE Photovoltaic Specialists Conference, New York, June 20-25, 2010, p. 1834.
[10]A. Takata, R. Oshima, Y. Shoji, K. Akahane, and Y. Okada, in Conference Record of the 35th IEEE Photovoltaic Specialists Conference, New York, June 20-25, 2010, p. 1877.
[11]S. M. Hubbard, C. Plourde, Z. Bittner, C. G. Bailey, M. Harris, T. Bald, M. Bennett, D. V. Forbes, and R. Raffaelle, in Conference Record of the 35th IEEE Photovoltaic Specialists Conference, New York, 2010, p. 1217.
[12]C. G. Bailey, D. V. Forbes, R. P. Raffaelle, and S. M. Hubbard, Appl. Phys. Lett. **98**, 163105 (2011).
[13]H. R. Stuart and D. G. Hall, Appl. Phys. Lett. **69**, 2327 (1996).
[14]V. E. Ferry, J. N. Munday, and H. A. Atwater, Adv. Mater. **22**, 4794 (2010).
[15]H. A. Atwater and A. Polman, Nat Mater **9**, 205 (2010).
[16]K. R. Catchpole and A. Polman, Opt. Express **16**, 21793 (2008).
[17]K. Nakayama, K. Tanabe, and H. A. Atwater, Appl. Phys. Lett. **93**, 121904 (2008).
[18]D. Derkacs, W. V. Chen, P. M. Matheu, S. H. Lim, P. K. L. Yu, and E. T. Yu, Appl. Phys. Lett. **93**, 091107 (2008).
[19]S. H. Lim, W. Mar, P. Matheu, D. Derkacs, and E. T. Yu, J. Appl. Phys. **101**, 104309 (2007).
[20]F. J. Beck, A. Polman, and K. R. Catchpole, J. Appl. Phys. **105**, 114310 (2009).
[21]M. Meier and A. Wokaun, Opt. Lett. **8**, 581 (1983).
[22]G. Xu, M. Tazawa, P. Jin, S. Nakao, and K. Yoshimura, Appl. Phys. Lett. **82**, 3811 (2003).
[23]F. J. Beck, S. Mokkapati, A. Polman, and K. R. Catchpole, Appl. Phys. Lett. **96**, 033113 (2010).
[24]K. R. Catchpole and A. Polman, Appl. Phys. Lett. **93**, 191113 (2008).
[25]E. Yablonovitch, J. Opt. Soc. Am. **72**, 899 (1982).
[26]W. G. Spitzer and J. M. Whelan, Phys. Rev. **114**, 59 (1959).